Am J Transl Res 2019;11(11):7157-7165
www.ajtr.org /ISSN:1943-8141/AJTR0101222

*Original Article*

# Comparison of anesthesia and tumor implantation methods for establishing rabbit VX2 hepatocarcinoma

Jiayi Liu*, Yanhui Li*, Jie Zhang, Yeyu Cai, Quanliang Shang, Cong Ma, Dujun Bian, Zhu Chen, Enhua Xiao

*Department of Radiology, The Second Xiangya Hospital of Central South University, Changsha, Hunan, China. *Equal contributors.*

Received August 20, 2019; Accepted November 11, 2019; Epub November 15, 2019; Published November 30, 2019

**Abstract:** In this study, we compared different anesthesia and operation methods for modeling VX2 hepatocarcinoma in rabbits. Forty New Zealand white rabbits were randomly divided into three groups: A, B, and C. Group A underwent ultrasound-guided implantation and intravenous anesthesia; Group B underwent ultrasound-guided implantation and inhalation anesthesia; Group C underwent laparotomy implantation and intravenous anesthesia. Anesthesia and operation differences were compared between groups A and B, and A and C, respectively. We used magnetic resonance imaging (MRI) to assess tumor formation and growth, and pathological examination and immunohistochemistry to confirm the biological characteristics of the specimens. The anesthetic preparation and postoperative resuscitation times were shorter in group A compared to group B; there were no significant between-group differences in the intraoperative satisfactory effect rate or mortality rate. The operation time, incision length, hemorrhage volume, and leukocyte counts were lower in group A than group C; there were no significant between-group differences in the postoperative infection rate or mortality rate. MRI revealed that the celiac implantation rate decreased dramatically in groups A and B; there were no significant between-group differences in the largest tumor diameter, tumorigenesis rate, intrahepatic multifocal implantation rate, or abdominal wall invasion rate. Ten samples were confirmed by pathological examination and immunohistochemistry to have VX2 tumors. To conclude, using an inhalation-based anesthetic method is beneficial for improving the efficiency of the VX2 tumor implantation operation. Compared with laparotomy implantation, ultrasound-guided implantation required less operation time, had lower levels of internal damage, and had a lower celiac implantation rate.

**Keywords:** Hepatocarcinoma, animal model, VX2, ultrasound, laparotomy, implantation

## Introduction

The rabbit VX2 tumor is a fundamental part of the animal model of hepatocellular carcinoma, as its blood supply and rapid growth simulates human hepatocarcinoma well. Thus, this model has been frequently used in studies on the therapeutic, diagnostic, and pathogenetic aspects of hepatocarcinoma [1-3]. Up until now, the rabbit VX2 hepatocarcinoma model has been developed using various techniques ranging from indirect to direct implantation, from cell suspension implantation to tissue fragment implantation [4, 5], and from invasive to noninvasive techniques [6, 7].

Currently, the two most widely used methods for developing the rabbit VX2 hepatocarcinoma model are traditional open surgery and ultrasound-guided percutaneous surgery with tumor tissue fragments; both of which have high rates of tumorigenesis. Although some studies have compared these two methods, they have some limitations, including not having specific time recordings, limited evaluation of tumor formation and metastasis, and limited quantitative analysis of the operation. Therefore, a detailed comparison of the application of these two methods is warranted.

In this study, we designed a detailed experimental protocol to quantitatively compare these two methods, and aimed to identify a more convenient method for the implantation of VX2 tumors.

## Materials and methods

The experimental protocol was approved by the Animal Care Committee at the Second Xiangya

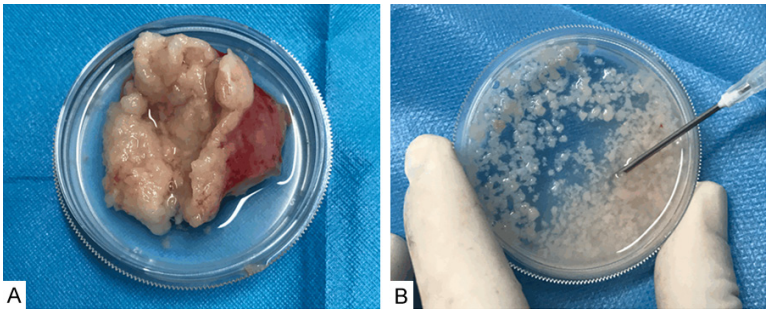

**Figure 1.** VX2 tumors extraction. A. Tumor tissue isolation: after removal of the necrotic tissue around the tumor, fish-like tumors were soaked in phosphate buffered solution. B. Segmentation: The tumor fragments were respectively drawn off with a 1-ml syringe until they were injected into the recipient rabbit's liver.

Hospital of Central South University (SYXK-2017-0002), and all animal experiments were carried out in strict accordance with the institutional guidelines. Maximum efforts were made to ensure that the operations were performed in a way that minimized animal suffering.

*Experimental animals and tumors*

In this study, we used 40 New Zealand white rabbits of both sexes weighing between 2.5 kg and 3.0 kg that were provided by the Experimental Animal Center of the Second Xiangya Hospital of Central South University. The VX2 tumor tissues which were inoculated into the hind limbs were donated by Union Hospital, which is affiliated with the Tongji Medical College of Huazhong University.

*VX2 tumors extraction*

Rabbits with hind limb tumors were anesthetized by intravenous injection of a 3% pentobarbital sodium solution (Sigma, CAS: 57-33-0, USA) using a 24 G detaining needle (BD, 0.7× 19 mm, B-9140 Temse, Belgium) via an ear vein. Under aseptic conditions, the tumors were removed from the surrounding tissue and cleaned, and the hind limb incision was sutured. Next, the tumors were placed in phosphate-buffered solution (HyClone, SH40007.01, UT, USA) to remove any fibers and wash out necrotic tissues.

The collected tumors were cut into small pieces (0.5-1 mm diameter) and stored in phosphate-buffered solution. Subsequently, the tumor tissue fragments were drawn up with a 1-ml syringe and injected into the recipient rabbit's liver (**Figure 1**).

*Anesthesia and preoperative preparation*

The 40 rabbits were randomly divided into three groups using a simple random sampling method: group A (ultrasound-guided implantation + intravenous anesthesia, 15 rabbits); group B (ultrasound-guided implantation + inhalation anesthesia, 10 rabbits); and group C (laparotomy implantation + intravenous anesthesia, 15 rabbits).

The experimental rabbits were routinely fasted with *ad libitum* access to water and underwent a physical examination prior to the operation to assess their health. Rabbits in group A and C were fixed in an animal fixator and anesthetized with an intravenous injection of 45 mg/kg pentobarbital sodium solution via an ear vein. Rabbits in group B were also first fixed and then anesthetized using isoflurane (Lunan better pharmaceutical, Shandong, China) through an inhalational anesthetic device (Friends Honesty Life Sciences Company Limited, AS-01-007, Beijing, China) that maintained an 800 ml/min oxygen flow and 2% isoflurane inhalational concentration. After losing the righting and limb withdrawal reflexes in response to a toe pinch, they were placed on a rabbit holder in the supine position, and the skin on the epigastrium was prepared.

*Laparotomy and ultrasound-guided implantation of VX2 tumors*

Under aseptic conditions, rabbits in group A and B underwent pre-operative preparation (as mentioned above) and then ultrasound-guided percutaneous implantation. A preliminary ultrasound (Mindray M9, Shenzhen, China) with an L12-4s transducer as the imaging guidance tool was used throughout the operation. First, the entire liver was observed using an abdominal ultrasound to evade important blood vessels, and to confirm the thickest area or edge between the two left lobes of the liver as the target implantation site. Next, a 16 G hollow

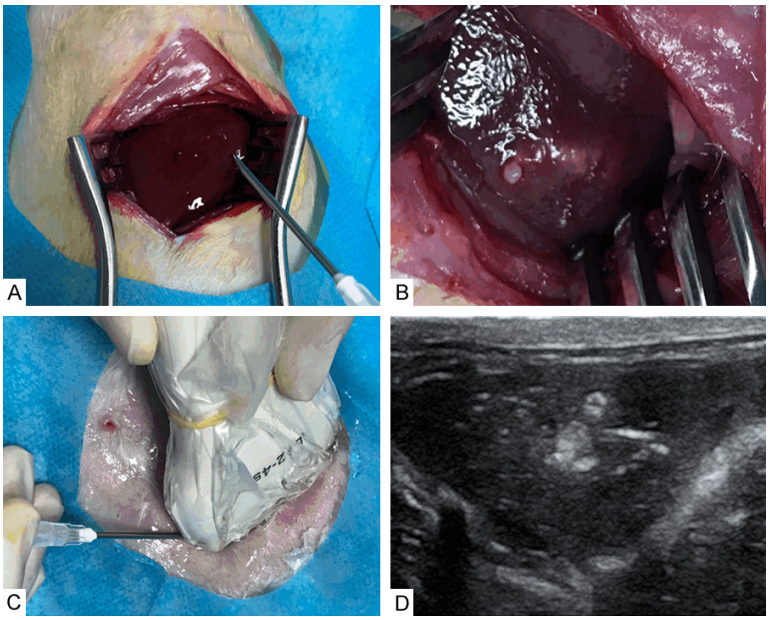


**Figure 2.** Laparotomy and ultrasound guided implantation of VX2 tumors. A. Laparotomy implantation process: The surface of the left lobe was punctured by a 16 G hollow needle, then about 0.5 ml of tumor fragments were injected. B. Laparotomy implantation evaluation: The success of implantation was confirmed by the surface of the liver becoming white and then the needle was removed. C. Ultrasound-guided implantation process: the target implantation site was confirmed through ultrasound-guided images. D. Ultrasound-guided implantation evaluation: when a focus of hyperechogenicity was seen and active bleeding was unseen, the success of implantation was confirmed.

needle (Ande medical company, 1.6×35 mm, Shandong, China) connected to a syringe filled with approximately 0.5 ml of tumor fragments was inserted into the predetermined location under ultrasound guidance and the tumor fragments in the syringe were injected. The success of the implantation procedure was confirmed when a hyperechoic focus was seen. Rabbits in group C underwent laparotomy surgery. In this procedure, the abdominal cavity was opened via a vertical incision using the subxiphoid approach, and the left lobe of the liver was exposed using a chest expander. The thickest area of the left lobe was confirmed as the puncture point through observation using smooth forceps. The surface of the left lobe was punctured using a 16 G hollow needle (as mentioned above), and approximately 0.5 ml of the tumor fragments were injected. The success of implantation was confirmed when the surface of the liver became white, after which the needle was removed. The incision was closed after confirming that there was no active hemorrhage (**Figure 2**).

*Intraoperative measurements*

The anesthetic preparation time was defined as the time elapsed between the infusion of the anesthetic drugs into a syringe or the inhalational apparatus of the anesthetic device to the loss of righting and limb withdrawal reflexes in response to toe pinch. The intraoperative depth of anesthesia was evaluated using the Richmond Agitation-Sedation Scale (RASS) [8]. An RASS score greater than 4 (response to physical stimuli) or death of the rabbit during the operation indicated a dissatisfactory anesthetic effect. For group A, the operation time was defined as the time elapsed from the start of the incision to the end of suturing. For group B, the operation time was defined as the time elapsed from the start of implantation site orientation to the end of needle withdrawal. The hemorrhage volume during the operation was calculated using precise weighing equipment (Mettler toledo, ME2002E, Zurich, Switzerland) to compare weight differences of the medical gauzes. Every medical gauze used during operation was placed in a sealed bag and weighed before starting the operation. After the surgery, each corresponding medical gauze was placed in a sealed bag and weighed again (as mentioned above). The weight difference was considered to be the hemorrhage volume. After stitching the incision, the incision length (cm) was measured.

*Postoperative measurements*

The postoperative resuscitation time was defined as the time elapsed from the end of the operation to when each rabbit could make conscious limb movements. Postoperative infection was determined by observing suppurative manifestation along the suture line or the puncture site within 2 weeks after operation. The inflammatory index was determined by calculat-

ing the number of leukocytes using a leukocyte counter (Beckman coulter, DxH 600 Coulter, Kraemer Boulevard Brea, USA) within 3 days after operation. Mortality was defined as death within 2 weeks and was recorded for all experimental rabbits. MRI assessment and pathological examination were used to determine the success rate of tumor implantation and tumor invasion or metastasis.

*MRI assessment*

Whole-body MRI assessment was performed 2 weeks after operation for all experimental rabbits using a 3.0 Tesla MRI system (Siemens Healthcare GmbH, MAGNETOM Skyra, München, Germany) and a 15 Ch phased-array torso coil (MDSS GmbH, Schiffgraben, Hannover, Germany). The MRI protocol included: (1) unenhanced T2-weighted fast spin-echo sequence (slice thickness, 3 mm; repetition time/echo time, 3940/109 ms; receiver bandwidth, 221 kHz) and (2) unenhanced and enhanced after an intravenous injection of 0.2 ml/kg of gadopentetate dimeglumine (Bayer, Magnevist, Berlin, Germany)] T1-weighted fast gradient-echo sequence (slice thickness, 4 mm; repetition time/echo time, 4/2 ms; receiver bandwidth, 450 kHz) in the arterial phase (10 s) and delayed phase (60 s). Three radiologists (Shang, Ma, and Bian), with more than 5 years of experience with abdominal diagnosis independently analyzed the images. Successful implantation was confirmed when the radiologists had unified opinions. The specific evaluation criteria were as follows: intrahepatic nodules or space-occupying masses after MRI scanning without contrast, appearance of marked enhancement during the arterial phase (20 s) after the injection of contrast, gradual vanishing or decrease of the tumor enhancements during the delayed phase (3 min). Tumor invasion and metastasis were also assessed using MRI.

*Pathological examination and immunohistochemistry (IHC)*

Any disagreements regarding suspicious signs during the discussions of MRI images of the implanted tumors and sampled specimens diagnosed with VX2 tumor after MRI assessment were resolved by pathological examination and immunohistochemistry. Moreover, rabbits whose health was too weak to undergo an MRI examination were euthanized, and pathological examination and immunohistochemistry were then performed. The suspected tumors in the liver were excised. Next, the specimens were soaked in a 10% paraformaldehyde solution within 48 hours, sectioned, fixed using paraffin, and stained with hematoxylin-eosin (HE). Immunohistochemistry was performed to examine epithelial cell and gland epithelial marker expression to confirm that the tissue origin was in agreement with the characteristics of VX2s. Briefly, the sections were blocked using 3% $H_2O_2$ in methanol and then incubated with 8% skimmed milk at 37°C for 30 min. The sections were then washed and incubated with anti-high molecular weight cytokeratin (Dako, anti-HCK, Glostrup, Denmark) and anti-cytokeratin 18 (Progen Biotechnik, anti-CK18, Frankfurt, Germany) at 4°C overnight for approximately 16 hours. They were then incubated with the secondary antibody (Zhongshan Golden Bridge, Beijing, China) at 37°C for 40 min. Next, the sections underwent chromogen treatment with 3,3'-diaminobenzidine (Zhongshan Golden Bridge, DAB, Beijing, China) for 5 min and were counterstained with Mayer's hematoxylin. Finally, the sections were dehydrated in gradient alcohol and sealed in resins. Cell clusters with brown-stained cytoplasm indicated a positive result.

*Data analysis*

Statistical analyses were performed using SPSS version 22.0 (SPSS, Inc, Chicago, IL, USA). Continuous data are presented as mean ± standard deviation, and dichotomous data are presented as n (%). The Chi-square goodness of fit test was used to examine differences in the dichotomous variables. When the number of samples was less than 40, or if the *p*-value obtained from the chi-square test was close to the α level, Fisher's exact tests were used instead. Student's *t*-tests were used to examine differences in continuous variables between groups. *P*-values <0.05 were considered to be statistically significant.

## Results

*Comparison of anesthesia differences*

The anesthetic preparation time was significantly shorter in group A (ultrasound-guided implantation + intravenous anesthesia, 15 rab-

**Table 1.** Comparison of anesthesia differences

| | Inhalation anesthesia | Intravenous anesthesia | t test | *p* value |
|---|---|---|---|---|
| Number of rabbits (n) | 10 | 15 | | |
| Weight (kg) | 2.70±0.11 | 2.75±0.74 | 1.21 | 0.24 |
| Anesthetic preparation time (s) | 96.80±12.1 | 522.67±104.1 | 12.79 | <0.001 |
| Postoperative resuscitation time (min) | 3.80±1.47 | 88.93±12.52 | 21.25 | <0.001 |
| Dissatisfactory effect number of anesthesia (n) | 0 | 3 | | |
| Satisfactory effect number of anesthesia (n) | 10 | 12 | | |
| Intraoperation satisfactory effect rate (%) | 100.0 | 80.0 | | 0.25 |
| Mortality number (n) | 0 | 0 | | |
| Survival number (n) | 10 | 15 | | |
| Mortality rate (%) | 0 | 0 | | 1.00 |

**Table 2.** Comparison of operation differences

| | US-guided implantation | Laparotomy implantation | t test | *p* value |
|---|---|---|---|---|
| Number of rabbits (n) | 15 | 15 | | |
| Weight (kg) | 2.74±0.07 | 2.74±0.08 | 0.45 | 0.66 |
| Operation time (min) | 5.01±1.39 | 20.00±3.67 | 14.76 | <0.001 |
| Volume of hemorrhage (ml) | 0 | 2.05±1.11 | 7.18 | <0.001 |
| Incision length (cm) | 0 | 3.73±1.06 | 13.62 | <0.001 |
| Leukocyte ($\times 10^9$/L) | 9.20±0.95 | 12.67±3.63 | 3.6 | 0.001 |
| Postoperative infection number (n) | 0 | 4 | | |
| Postoperative non-infection number (n) | 15 | 11 | | |
| Postoperative infection rate (%) | 0.0 | 26.7 | | 0.10 |
| Mortality number (n) | 0 | 3 | | |
| Survival number (n) | 15 | 12 | | |
| Mortality rate (%) | 0.0 | 20.0 | | 0.22 |

bits) than in group B (ultrasound-guided implantation + inhalation anesthesia, 10 rabbits). On the other hand, the postoperative resuscitation time was significantly shorter in group B compared to group A. Three rabbits in group A showed a dissatisfactory anesthetic effect, while none in group B did. No rabbits in either groups A or B died during the operation. There were no significant between-group differences in the intraoperative satisfactory effect rate or mortality rate (**Table 1**).

*Comparison of operation differences*

The operation time and incision length were significantly shorter in group A compared to group C (laparotomy implantation + intravenous anesthesia, 15 rabbits). The hemorrhage volume and leukocyte counts were significantly lower in group A compared to group C. No infections were observed in group A within 2 weeks after surgery, whereas four rabbits in group C developed an incision infection accompanied by suppurative manifestation and a high leukocyte count within 2 weeks after surgery. Within 2 weeks after surgery, no rabbits died in group A, while 3 died in group C. Autopsy examinations revealed abdominal infection. There were no significant between-group differences in the postoperative infection rate or mortality rate (**Table 2**).

*MRI assessment*

The remaining 12 rabbits in group C and 25 rabbits in groups A and B underwent MRI examination to assess the characteristics of tumor formation and tumorigenesis rate. Eleven of the twelve rabbits in group C and 24 of the 25 rabbits in groups A and B underwent successful implantation (**Figure 3**). Ten of the twelve rabbits in group C and 19 of the 25 rabbits in groups A and B had tumor necrosis. Two of the twelve rabbits in group C, and 3 of the 25 rab-

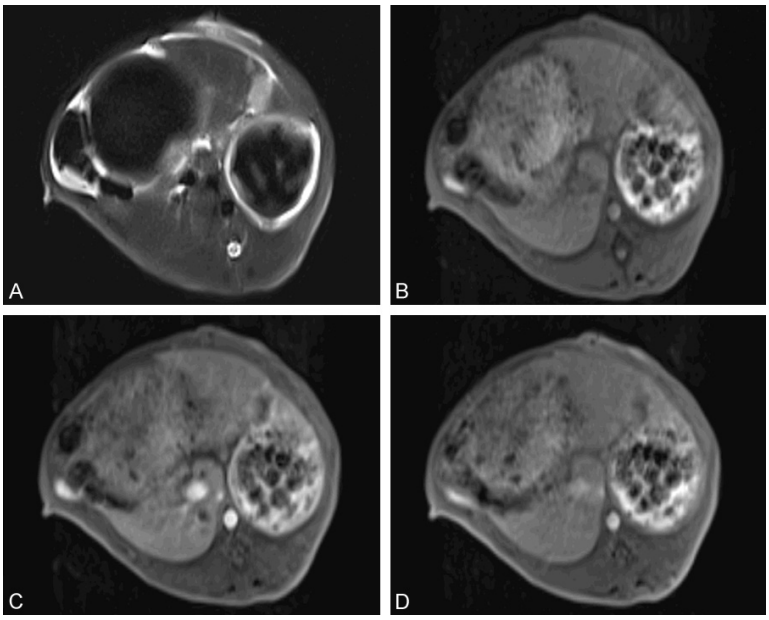


**Figure 3.** MRI detection of successfully implanted VX2 hepatocarcinoma. (A) T2-weighted images and (B) T1-weighted images: single intrahepatic nodules could see in figures. The T2-weighted images showed more distinct boundary than that of T1-weighted images. (C) T1-weighted enhanced images at the arterial phase: marked enhancement on implantation site showed a similar radiological performance to hepatocarcinoma. (D) T1-weighted enhanced images at the delayed phase: vanished appearances on implantation site were also similar to the performance of hepatocarcinoma.

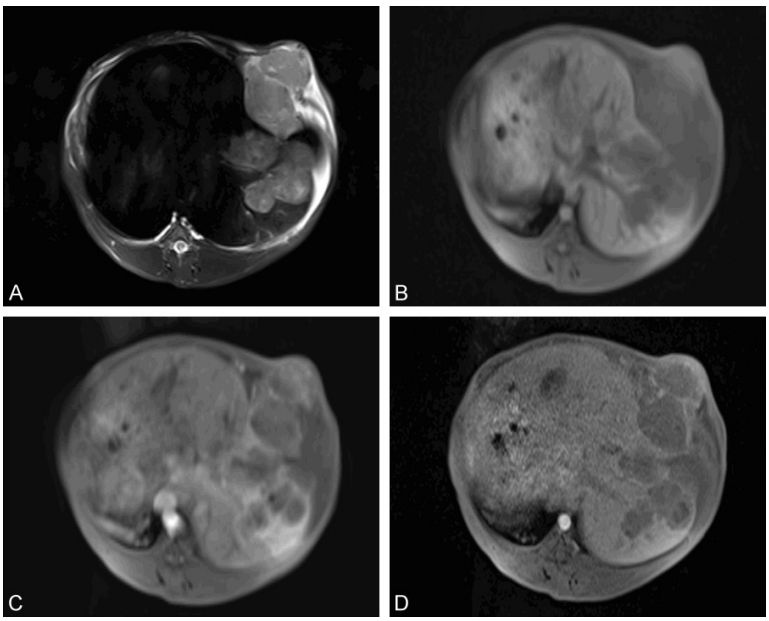


**Figure 4.** MRI detection ofVX2 hepatocarcinoma with intrahepatic multifocal implantation and abdominal wall invasion. (A) T2-weighted images and (B) T1-weighted images: intrahepatic multifocal nodules and abdominal wall nodules. (C) T1-weighted enhanced images at the arterial phase: marked enhancement on implantation site and abdominal wall demonstrated that multifocal nodules and abdominal wall nodules were VX2 hepatocarcinoma with hypervascular pattern. (D) T1-weighted enhanced images at the delayed phase: vanished appearances on implantation site and abdominal wall could also illustrate the similar performance of hepatocarcinoma.

bits in groups A and B had intrahepatic multifocal implantation. Three of the twelve rabbits in group C, and 3 of the 25 rabbits in groups A and B had abdominal wall invasion (**Figure 4**). Four of the twelve rabbits in group C, and 1 of the 25 rabbits in groups A and B had typical signs of celiac implantation (**Figure 5**). There was a dramatic decrease in the celiac implantation rate in group C. There were no significant between-group differences regarding decreases in the largest tumor diameter, tumorigenesis rate, intrahepatic multifocal implantation rate, or abdominal wall invasion rate (**Table 3**).

*Pathological examination and immunohistochemistry*

Three rabbits died prior to MRI assessment, two showed signs of an abscess or had an indefinite tumor location due to abdominal infection, and five had VX2 tumors after MRI assessment. A total of 10 samples underwent pathological examination and immunohistochemistry. We used conventional HE staining and squamous and glandular epithelium markers for tumor detection. We found that all of the liver specimens had VX2 hepatocarcinoma, including high magnificence in HE staining, and HCK high magnificence and CK18 low magnificence with IHC staining. Histologically, we confirmed that our animal models had squamous cell hepatocarcinoma (**Figure 6**).

## Discussion

Intravenous anesthesia is commonly used to establish the VX2 rabbit hepatocarcino-

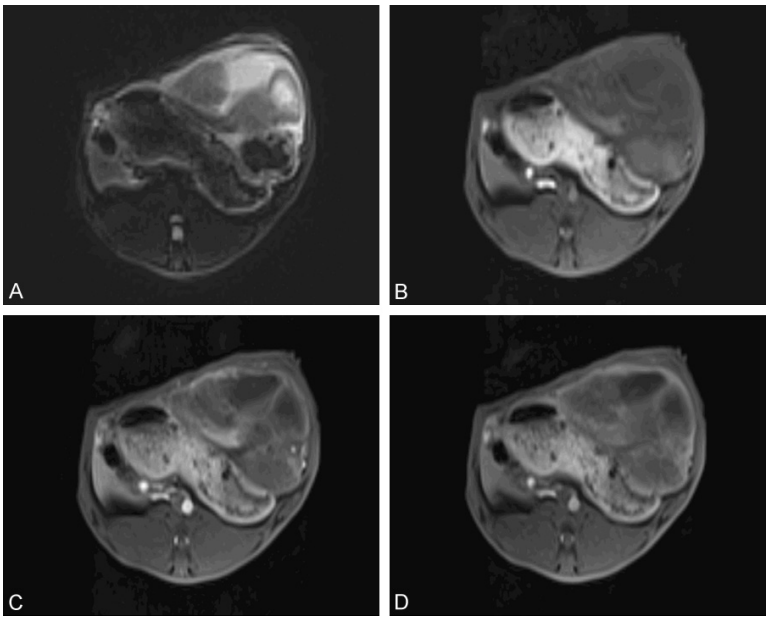


**Figure 5.** MRI detection of VX2 hepatocarcinoma with celiac implantation. (A) T2-weighted images and (B) T1-weighted images: celiac implantation. (C) T1-weighted enhanced images at the arterial phase: marked enhancement demonstrated that VX2 hepatocarcinoma implanted in celiac. (D) T1-weighted enhanced images at the delayed phase: mild enhancement revealed that VX2 tumor in celiac had less blood supplying than other implantation site.

ma model. However, the venipuncture and irregular stimulus reflex in animals disrupts the anesthesia process. For example, these factors can impair the operators, result in multiple injections of anesthetic drugs, and waste operation time. Isoflurane is an inhalation-based anesthetic drug that rapidly induces anesthesia and requires less postoperative resuscitation time. Additionally, its performance does not involve contact with the animal. To the best of our knowledge, this is the first study to compare inhalation and intravenous anesthetic methods for establishing the rabbit VX2 hepatocarcinoma model. We found that inhalation anesthesia required far less anesthetic preparation time and postoperative resuscitation time than intravenous anesthesia. Therefore, its application could help to reduce the total operation time.

Previous studies have used many modified methods of laparotomy implantation or ultrasound-guided implantation for modeling rabbit VX2 hepatocarcinoma. Regarding laparotomy implantation, Virmani and colleagues [9] recommended that laparotomy implantation of freshly harvested VX2 tumor fragments into the liver parenchyma is better than injecting a cell suspension of the VX2 tumor. Chen and colleagues [5] modified the implantation method by injection rather than by building a sinus using tweezers. Regarding ultrasound-guided implantation, white and colleagues [10] confirmed that it can safely provide reliable tumor growth. These changes have greatly increased the success rate of VX2 liver tumor implantation. In our study, we adopted the advantages that were discovered by previous studies, and compared the two methods in detail. We found that ultrasound-guided implantation in rabbits involved less time and internal damage than laparotomy implantation in terms of the operation time, hemorrhage volume, incision length, and postoperative leukocyte count. There were no significant differences in the rates of postoperative infection or mortality between the two methods. Both implantation methods showed a high success rate, which can be attributed to the procedures being performed with direct visual observation and fresh tumor fragments. There were significant between-method differences in the celiac implantation rates. This may be due to the fact that although the puncture point of the liver was observed, the depth was unclear, which may have led to the leakage of tumor fragments into the space between the two left lobes of the liver. Further, abdominal wall invasion may have been caused by the shallow depth of tumor implantation.

MRI is a commonly used, reliable method to evaluate tumor formation, including the configuration of the vascular, functional, and anatomical characteristics. Previous studies have used MRI to assess growth changes of VX2 tumors [11-13]. In our study, we used the characteristic rich blood supply of the VX2 tumors to assess the arterial and delayed phases. We found a high level of consistency between the imaging and pathological findings. Thus, the formation

**Table 3.** Comparison of MRI detection between two different operative methods

| | US-guided implantation | Laparotomy implantation | t test | *p* value |
|---|---|---|---|---|
| Number of rabbits (n) | 25 | 12 | | |
| Largest tumor diameter (cm) | 1.63±0.29 | 1.50±0.20 | 1.38 | 0.18 |
| Successfully implanted (n) | 24 | 11 | | |
| Unsuccessfully implanted (n) | 1 | 1 | | |
| Successful implantation rate (%) | 96.0 | 91.7 | | 1.00 |
| No tumor necrosis(n) | 6 | 2 | | |
| With tumor necrosis (n) | 19 | 10 | | |
| Tumor necrosis rate (%) | 76.0 | 83.3 | | 1.00 |
| No multifocal intrahepatic implantation (n) | 22 | 10 | | |
| Intrahepatic multifocal implantation (n) | 3 | 2 | | |
| Intrahepatic multifocal implantation rate (%) | 12.0 | 16.7 | | 1.00 |
| No abdominal wall invasion (n) | 22 | 9 | | |
| With abdominal wall invasion (n) | 3 | 3 | | |
| Abdominal wall invasion rate (%) | 12.0 | 25.0 | | 0.37 |
| No celiac implantation (n) | 24 | 8 | | |
| With celiac implantation (n) | 1 | 4 | | |
| Celiac metastasis rate (%) | 4.0 | 33.3 | | 0.03 |

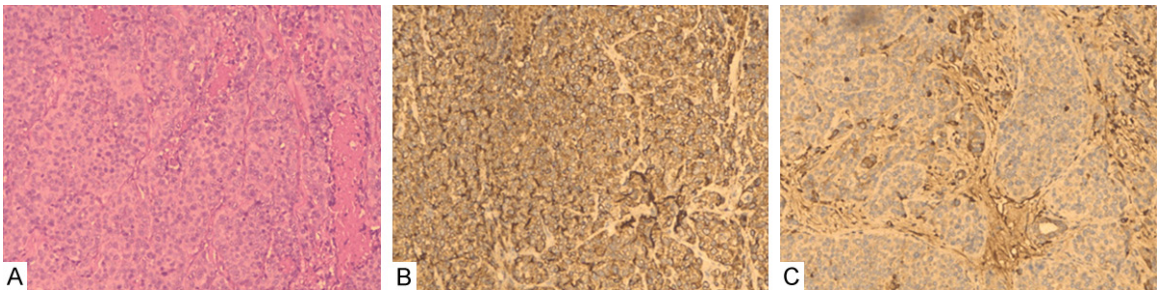


**Figure 6.** Pathological examination and immunohistochemistry (IHC). A. HE staining (100×): the morphology of VX2 tumor cells. B. IHC staining of an epithelial cell marker, HCK (100×): positive expression indicated by the brown signals. C. IHC staining of a gland epithelial marker, CK18 (100×): negative expression showed unstained tumor cells.

of the VX2 tumor can be well-evaluated using MRI arterial phase enhancement examination, which has a certain degree of reliability. There was a significantly high proportion of tumor necrosis with both operation methods. One potential explanation is that the tumor necrosis was associated with the tumor characteristics since the solid part of the tumor is often accompanied by abscess formation. We also considered that, given the high success rate of VX2 tumor implantation, the injection of 0.5 ml of tumor fragments was likely excessive, thus increasing the rate of abscess formation. Further studies are required to determine if the injection of fewer tumor fragments can reduce the rate of tumor necrosis. Immunohistochemistry results showed that the VX2 tumors originated from epithelial tissue. Further, the tumors showed obvious characteristics of epithelial tissue, which is consistent with the previous findings of a study on virus-induced papilloma in rabbits [14].

One limitation of our study was the small sample size (n=40), which may have impacted the statistical power. Additionally, an integrated analysis would likely improve the utilization efficiency of the samples. In conclusion, we found that altering the anesthetic method could be beneficial for improvement of the efficiency of the VX2 tumor implantation operation. Compared with laparotomy implantation, ultrasound-guided implantation requires less operation time, and has lower levels of internal damage and celiac implantation.

## Acknowledgements

This study was supported by National Natural Science Foundation of China (Nos. 81601471; 81571784; 30870695), Provincial Natural Science Foundation of Hunan (Nos. 2019JJ40434; 2019JJ40444; 2018JJ2578), Scientific Research Project of Hunan Health and Family Planning Commission (No. B20180048).

## Disclosure of conflict of interest

None.

**Address correspondence to:** Drs. Enhua Xiao and Zhu Chen, Department of Radiology, The Second Xiangya Hospital of Central South University, Changsha 410011, Hunan, China. Tel: +86-13054187080; E-mail: xiaoenhua64@csu.edu.cn (EHX); Tel: +86-13875930094; E-mail: chenzhu415@csu.edu.cn (ZC)

## References

[1] Lv P, Liu J, Yan X, Chai Y, Chen Y, Gao J, Pan Y, Li S, Guo H and Zhou Y. CT spectral imaging for monitoring the therapeutic efficacy of VEGF receptor kinase inhibitor AG-013736 in rabbit VX2 liver tumours. Eur Radiol 2017; 27: 918-926.

[2] Park W, Gordon AC, Cho S, Huang X, Harris KR, Larson AC and Kim DH. Immunomodulatory magnetic microspheres for augmenting tumor-specific infiltration of natural killer (NK) cells. ACS Appl Mater Interfaces 2017; 9: 13819-13824.

[3] Chen Z, Xiao EH, Kang Z, Zeng WB, Tan HL, Li HB, Bian DJ and Shang QL. In vitro and in vivo magnetic resonance imaging with chlorotoxin-conjugated superparamagnetic nanoprobes for targeting hepatocarcinoma. Oncol Rep 2016; 35: 3059-3067.

[4] Sun JH, Zhang YL, Nie CH, Yu XB, Xie HY, Zhou L and Zheng SS. Considerations for two inoculation methods of rabbit hepatic tumors: pathology and image features. Exp Ther Med 2012; 3: 386-390.

[5] Chen Z, Kang Z, Xiao EH, Tong M, Xiao YD and Li HB. Comparison of two different laparotomy methods for modeling rabbit VX2 hepatocarcinoma. World J Gastroenterol 2015; 21: 4875-4882.

[6] Lee KH, Liapi E, Buijs M, Vossen JA, Prieto-Ventura V, Syed LH and Geschwind JF. Percutaneous US-guided implantation of Vx-2 carcinoma into rabbit liver: a comparison with open surgical method. J Surg Res 2009; 155: 94-99.

[7] Luo W, Zhou X, Zheng X, He G, Yu M, Li Q and Liu Q. Role of sonography for implantation and sequential evaluation of a VX2 rabbit liver tumor model. J Ultrasound Med 2010; 29: 51-60.

[8] Sessler CN, Gosnell MS, Grap MJ, Brophy GM, O'Neal PV, Keane KA, Tesoro EP and Elswick RK. The richmond agitation-sedation scale: validity and reliability in adult intensive care unit patients. Am J Respir Crit Care Med 2002; 166: 1338-1344.

[9] Virmani S, Harris KR, Szolc-Kowalska B, Paunesku T, Woloschak GE, Lee FT, Lewandowski RJ, Sato KT, Ryu RK, Salem R, Larson AC and Omary RA. Comparison of two different methods for inoculating VX2 tumors in rabbit livers and hind limbs. J Vasc Interv Radiol 2008; 19: 931-936.

[10] White SB, Chen J, Gordon AC, Harris KR, Nicolai JR, West DL and Larson AC. Percutaneous ultrasound guided implantation of VX2 for creation of a rabbit hepatic tumor model. PLoS One 2015; 10: e0123888.

[11] Qi XL, Liu J, Burns PN and Wright GA. The characteristics of vascular growth in VX2 tumor measured by MRI and micro-CT. J Oncol 2012; 2012: 362096.

[12] Wang D, Virmani S, Tang R, Szolc-Kowalska B, Woloschak G, Omary RA and Larson AC. Four-dimensional transcatheter intraarterial perfusion (TRIP)-MRI for monitoring liver tumor embolization in VX2 rabbits. Magn Reson Med 2008; 60: 970-975.

[13] Liang XM, Tang GY, Cheng YS and Zhou B. Evaluation of a rabbit rectal VX2 carcinoma model using computed tomography and magnetic resonance imaging. World J Gastroenterol 2009; 15: 2139-2144.

[14] Moore DH, Stone RS, Shope RE and Gelber D. Ultrastructure and site of formation of rabbit papilloma virus. Proc Soc Exp Biol Med 1959; 101: 575-578.